Thyroid Receptor Ligands. 1. Agonist Ligands Selective for the Thyroid Receptor β_1

Liu Ye,[†] Yi-Lin Li,[†] Karin Mellström,[†] Charlotta Mellin,[†] Lars-Göran Bladh,[†] Konrad Koehler,[†] Neeraj Garg,[†] Ana Maria Garcia Collazo,[†] Chris Litten,[†] Bolette Husman,[†] Karina Persson,[†] Jan Ljunggren,[†] Gary Grover,[‡] Paul G. Sleph,[‡] Rocco George,[‡] and Johan Malm[†,*]

Karo Bio AB, Novum, Huddinge S-141 57, Sweden, and Metabolic and Cardiovascular Drug Discovery, Bristol-Myers Squibb, Pharmaceutical Research Institute, Pennington, New Jersey 08543-2130

Received October 25, 2002

Endogenous thyroid receptor hormones 3,5,3′,5′-tetraiodo-L-thyronine (T_4, **1**) and 3,5,3′-triiodo-L-thyronine (T_3, **2**) exert a significant effects on growth, development, and homeostasis in mammals. They regulate important genes in intestinal, skeletal, and cardiac muscles, the liver, and the central nervous system, influence overall metabolic rate, cholesterol and triglyceride levels, and heart rate, and affect mood and overall sense of well being. The literature suggests many or most effects of thyroid hormones on the heart, in particular on the heart rate and rhythm, are mediated through the TRα_1 isoform, while most actions of the hormones on the liver and other tissues are mediated more through the TRβ_1 isoform of the receptor. Some effects of thyroid hormones may be therapeutically useful in nonthyroid disorders if adverse effects can be minimized or eliminated. These potentially useful features include weight reduction for the treatment of obesity, cholesterol lowering for treating hyperlipidemia, amelioration of depression, and stimulation of bone formation in osteoporosis. Prior attempts to utilize thyroid hormones pharmacologically to treat these disorders have been limited by manifestations of hyperthyroidism and, in particular, cardiovascular toxicity. Consequently, development of thyroid hormone receptor agonists that are selective for the β-isoform could lead to safe therapies for these common disorders while avoiding cardiotoxicity. We describe here the synthesis and evaluation of a series of novel TR ligands, which are selective for TRβ_1 over TRα_1. These ligands could potentially be useful for treatment of various disorders as outlined above. From a series of homologous R_1-substituted carboxylic acid derivatives, increasing chain length was found to have a profound effect on affinity and selectivity in a radioreceptor binding assay for the human thyroid hormone receptors α_1 and β_1 (TRα_1 and TRβ_2) as well as a reporter cell assay employing CHOK1-cells (Chinese hamster ovary cells) stably transfected with hTRα_1 or hTRβ_1 and an alkaline phosphatase reporter-gene downstream thyroid response element (TRAFα_1 and TRAFβ_1). Affinity increases in the order formic, acetic, and propionic acid, while β-selectivity is highest when the R_1 position is substituted with acetic acid. Within this series 3,5-dibromo-4-[(4-hydroxy-3-isopropylphenoxy)phenyl]acetic acid (**11a**) and 3,5-dichloro-4-[(4-hydroxy-3-isopropylphenoxy)phenyl]acetic acid (**15**) were found to reveal the most promising in vitro data based on isoform selectivity and were selected for further in vivo studies. The effect of **2**, **11a**, and **15** in a cholesterol-fed rat model was monitored including potencies for heart rate (ED_{15}), cholesterol (ED_{50}), and TSH (ED_{50}). Potency for tachycardia was significantly reduced for the TRβ selective compounds **11a** and **15** compared with **2**, while both **11a** and **15** retained the cholesterol-lowering potency of **2**. This left an approximately 10-fold therapeutic window between heart rate and cholesterol, which is consistent with the action of ligands that are approximately 10-fold more selective for TRβ_1. We also report the X-ray crystallographic structures of the ligand binding domains of TRα and TRβ in complex with **15**. These structures reveal that the single amino acid difference in the ligand binding pocket (Ser277 in TRα or Asn331 in TRβ) results in a slightly different hydrogen bonding pattern that may explain the increased β-selectivity of **15**.

Introduction

Nuclear hormone receptors comprise a class of intracellular, mostly ligand-regulated transcription factors, which include receptors for thyroid hormones. Thyroid hormones exert profound effects on growth, development, and homeostasis in mammals.[1] They regulate important genes in intestinal, skeletal, and cardiac muscles, liver, and the central nervous system, influence overall metabolic rate, cholesterol and triglyceride levels, and heart rate, and affect mood and overall sense of well being.

There are two major subtypes of the thyroid hormone receptors, α (TRα) and β (TRβ), expressed from two different genes. Differential RNA processing results in the formation of at least two isoforms from each gene.

* Corresponding author: Johan Malm, Karo Bio AB, Novum, S-141 57, Sweden. Tel: +46-8-608 6046; Fax: +46-8-774 8261; E-mail: johan.malm@karobio.se.
[†] Karo Bio AB.
[‡] Bristol-Myers Squibb.

10.1021/jm021080f CCC: $25.00
Published on Web 03/21/2003

The TRα_1, TRβ_1, and TRβ_2 isoforms bind thyroid hormone and act as ligand-regulated transcription factors. The TRα_2 isoform is prevalent in the pituitary and other parts of the central nervous system, does not bind thyroid hormones, and acts in many contexts as a transcriptional repressor. In adults, the TRβ_1 isoform is the most prevalent form in most tissues, especially in the liver. The TRα_1 isoform is also widely distributed, although its levels are generally lower than those of the TRβ_1 isoform. The literature suggests many or most effects of thyroid hormones on the heart, and in particular on the heart rate and rhythm, are mediated through the TRα_1 isoform. On the other hand, most actions of the hormones on the liver and other tissues are mediated more through the β-forms of the receptor.[4,5]

The three-dimensional structure of the ligand binding domain of several nuclear receptors have been determined.[6−11] The overall fold constitutes a mostly α-helical structure with a hormone binding pocket deeply buried within the interior of the protein. For the thyroid hormone receptor both α_1 and β_1 subtypes have been determined,[6,12,13] revealing a single amino acid difference in residues surrounding the ligand binding pocket.

Thyroid hormones are currently used primarily as replacement therapy for patients with hypothyroidism. Therapy with 3,5,3′,5′-tetraiodo-L-thyronine (T_4, **1**) and 3,5,3′-triiodo-L-thyronine (T_3, **2**) usually returns metabolic functions to the euthyroid state. Some effects of thyroid hormones may be therapeutically useful in nonthyroid disorders if adverse effects can be minimized or eliminated. These potentially useful features include weight reduction for the treatment of obesity,[14] cholesterol lowering to treat hyperlipidemia,[15−17] amelioration of depression, and stimulation of bone formation in osteoporosis. Prior attempts to utilize thyroid hormones pharmacologically to treat these disorders have been limited by manifestations of hyperthyroidism and, in particular, by cardiovascular toxicity. Consequently, development of thyroid hormone receptor agonists selective for the β_1-isoform could lead to specific therapies for these common disorders while avoiding cardiotoxicity.

We describe here the synthesis and evaluation of a number of novel TR-ligands, which are selective for TRβ_1 over TRα_1. These ligands could potentially be useful for treatment of various disorders as outlined above.

Design Principles

Although there is a large body of structure−activity data on thyroid hormones that highlight structural features for high-affinity TR-ligands[19] there are very few indications in the literature on how to achieve selectivity for TRβ_1 over TRα_1. It is evident that significant β_1-selectivity is yet to be demonstrated. However, even ligands with modest β_1-selectivity display pharmacological profiles that are significantly different from the natural ligand **2**. A synthetic ligand, 3,5-dimethyl-4-(4-hydroy-3-isopropylbenzyl)phenoxy acetic acid (GC-1), shows an 8-fold selectivity in binding for the β subtype over the α subtype and a more than 10-fold preference in transactivation.[20] In hypercholesteremic rats, GC-1, unlike **2**, lowers serum cholesterol and TSH at concentrations that do not affect heart rate.[21] The effects of long-term administration of 3,5,3′-triiodothyroacetic acid (TRIAC, **3**) on patients has been studied several times. As exemplified in one study, heart rate remained constant throughout the study while serum total cholesterol, triglyceride, and total lipid concentration was decreased.[22]

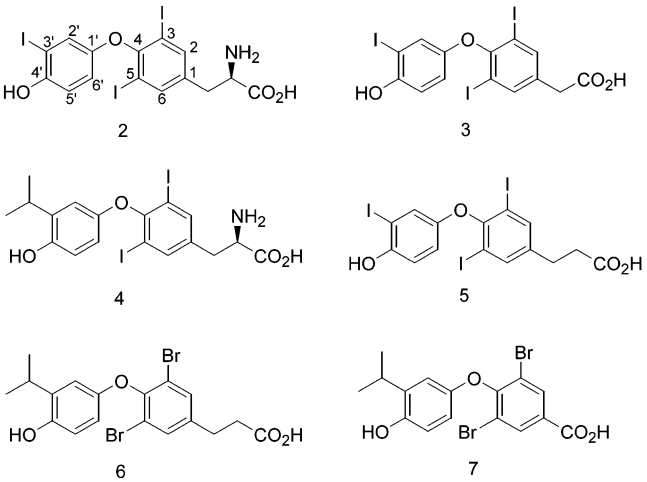

Figure 1. Structures of reported thyroid hormone ligands **2**−**7**. Ring numbering of **2** (T_3).

Table 1. Effects of Chronic Administration of Reported Thyromimetics on Thyroid Hormone Receptors

ID	TRα_1, IC_{50} [a]	TRβ_1	α_1/β_1, IC_{50} [a]
2	0.24	0.26	0.92
3	0.14	0.048	2.9
4	0.14	0.11	0.72
5	0.041	0.019	1.3
6	0.10	0.025	4.0
7	9.7	2.1	4.6

[a] IC_{50} values are calculated means from duplicate measurements and are expressed as nM. The variability of the measurements is on average ±25%. [b] Normalized ratio (see the Experimental Section for an explanation).

The aim of this investigation was to construct a structure−activity relationship comprising new ligands in order to elucidate the factors that are responsible for β_1-selectivity. Given the wealth of already reported ligands, we realized that examination of key ligands might provide a good starting point for the design of β_1-selective compounds. Consequently, the initial design was based on the comparison of **2**, 3,5,3′-triiodothyroacetic acid (**3**), 3,5-diiodo-3′-isopropyl-thyronine (**4**), L-3,5,3′-triiodothyropropionic acid (**5**), and 3,5-dibromo-4-(4-hydroxy-3-isopropylphenoxy)phenyl-propionic acid (**6**).[23] Furthermore, during the course of the writing of this manuscript the synthesis and evaluation of 3,5-dibromo-4-(4-hydroxy-3-isopropylphenoxy)benzoic acid (**7**) was published[24] (Figure 1).

From the results of a radioligand binding assay for the human TRα_1 and TRβ_1 (Table 1) a number of general conclusions concerning receptor affinity can be drawn: (i) affinity to both TRα_1 and TRβ_1 increases when the α-amino group of the alanine side-chain of **2** is replaced by a hydrogen atom as in **5**, (ii) the R_3′-iodine of **2** can be replaced by an isopropyl group as in **4** without any loss of activity; (iii) likewise R_3 and R_5 iodide atoms may be replaced by either bromine or chlorine and still retain high affinity for both receptor isoforms; (iv) significant loss of affinity is evident when

Scheme 1[a]

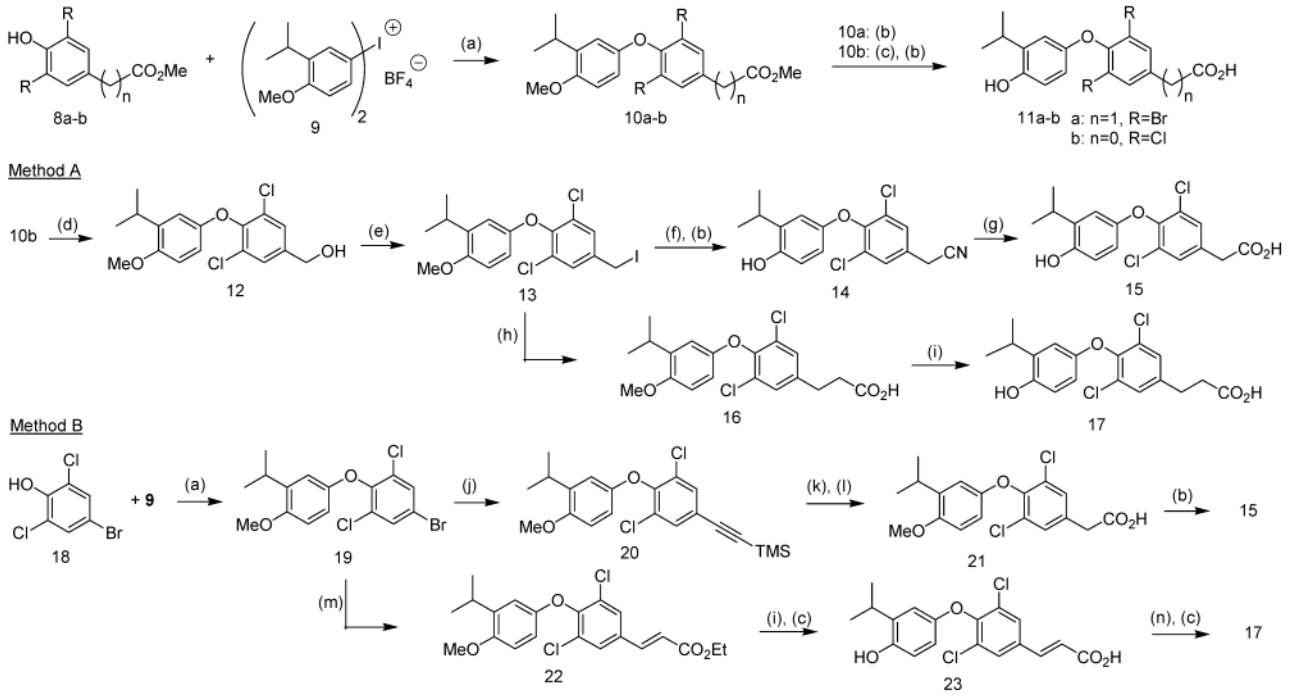

[a] Reagents and conditions: (a) Cu, Et_3N; CH_2Cl_2, RT; (b) BBr_3, CH_2Cl_2, 0 °C; (c) NaOH, MeOH, RT; (d) DIBAL, THF, RT; (e) P_2O_5, H_3PO_4, NaI, 120 °C; (f) NaCN, EtOH, H_2O, Δ; (g) AcOH, H_2SO_4, H_2O, 105 °C; (h) Na, *tert*-butyl alcohol, ethyl malonate, 90 °C; (i) BF_3−SMe_2, RT; (j) TMS-acetylene, $PdCl_2(PPh_3)_2$, CuI, TEA, 100 °C; (k) cyclohexene, BH_3−THF, RT; (l) NaOH, H_2O_2, 0 °C; (m) ethyl acrylate, $Pd(OAc)_2$, PPh_3, Et_3N, DMF, 100 °C; (n) H_2 (1 atm), PtO_2, MeOH, RT.

the side chain at the R_1-position is as short as benzoic acid (**7**). These findings confirm data already reported in the literature,[18] but also it appears to be general for both receptor isoforms. Concerning receptor isoform selectivity, there is a tendency that acetic (**3**) and benzoic (**7**), as opposed to a propionic acid (**5**) or an alanine side chain (**2**), favors β_1-selectivity. Furthermore, when the iodine atoms at the R_3-, R_5-, and R_3'-positions of **5** are replaced by bromine at the R_3- and R_5-positions and by isopropyl at the R_3'-position (**6**), β_1-selectivity increases 3-fold without any significant loss of affinity. An added advantage of replacing the iodines with alternative substituents is that analogue design might be less restricted. Iodines are highly susceptible to reductive deiodination and are also problematic upon biaryl ether formation due to its large steric bulk. Furthermore, with regard to achieve in vivo activity, replacing the iodines with alternative substituents eliminates the potential route of metabolic deactivation via enzymatic deiodination.

Results and Discussion

Chemistry. A series of thyromimetics, all varying the length of the carboxylic acid side chain at the R_1-position and the halogen substituents at the R_3- and R_5-positions was prepared as outlined in Scheme 1. Phenols **8a** and commercially available **8b** were coupled with bis(3-isopropyl-4-methoxyphenyl)iodonium tetrafluoroborate (**9**) following a previously reported method.[23] Alternative methods exist in the literature for the assembly of biaryl ethers,[25,26] but the present strategy was the most straightforward method when considering yields, availability of starting material, and the desired substitution pattern. The formed biaryl ether **10a** was treated with boron tribromide to give the final target compound **11a**, while **10b** was deprotected by saponification of the ester-function, followed by treatment of the free acid product with boron tribromide to give the end product **11b**.

The same strategy as above was attempted for the preparation of 3,5-dichloro-4-(4-hydroxy-3-isopropylphenoxy)phenylacetic acid (**15**) and 3,5-dichloro-4-(4-hydroxy-3-isopropylphenoxy)phenylpropionic acid (**17**) but with moderate success, as the required starting materials 3-(3,5-dichlorophenyl)acetic acid and 3-(3,5-dichlorophenyl)propionic acid were difficult to prepare via direct chlorination of the corresponding phenols. Several attempts were made but gave low yields of desired material or produced complex reaction mixtures mainly due to chlorination of the α-position in the carboxylic acid side chain.

Instead, **15** and **17** were prepared from **10b**, via a one- and two carbon homologation sequence, respectively (Method A). The ester was reduced to the alcohol (**12**) by treatment with diisobutyl aluminum hydride in THF. In the next step, sodium iodide was added to a mixture of **12**, P_2O_5, and H_3PO_4 and heated to give the iodide **13**. Deprotection followed by treatment with sodium cyanide gave the intermediate phenylacetonitrile **14**, which was hydrolyzed under basic conditions to give the end product **15**. The intermediate **13** could also be utilized for the preparation of **17**. The anion of ethyl malonate was reacted with **13**, hydrolyzed, and heated to give the corresponding monoacid **16**. Removal of the methyl ether-protecting group employing trifluoroboron dimethyl sulfide complex yielded the final product **17**. Total yields of **15** and **17** from available starting material **8b** was 18 and 2.4%, respectively.

Due to the low overall yields and time-consuming preparation, alternative routes based on palladium-catalyzed coupling reactions were explored (Method B).

Table 2. Effects of Chronic Administration of Synthetic Thyromimetics on Thyroid Hormone Receptors

ID	ThRα_1, IC_{50}(SD)[a]	ThRβ_1, IC_{50}(SD)[a]	α_1/β_1 [b]	TRAFα_1, EC_{50} [c]	TRAFβ_1, EC_{50} [c]	α_1/β_1
11a	1.4 (0.76)	0.095 (0.040)	8.7	0.38	0.20	1.9
11b	130 (48)	21 (9.0)	3.7	190	150	1.3
15	25 (2.9)	1.1 (0.051)	14	11	3.5	3.1
17	0.76 (0.25)	0.15 (0.025)	3.0	0.30	0.28	1.2

[a] IC_{50} values are expressed as nM and are calculated means of triplicate runs. SD = standard deviation. [b] Normalized ratio (see the Experimental Section for an explanation). [c] EC_{50} values are expressed as nM and are calculated means of duplicate runs. The variability of the measurements is on average ±25%.

Iodonium salt coupling with phenol **18** gave biaryl ether **19**. Application of the Sonagashira coupling of **19** with trimethylsilylacetylene gave the coupled product **20** regioselectively. Desilylation and subsequent oxidation employing hydrogen peroxide in the presence of base gave the phenylacetic acid **21**, which was demethylated as **10b** above. The total yield using the described sequence above is 28%, obviously less time-consuming and was the preferred method for large scale production of **15**. The intermediate bromo compound **19** could also be utilized to build a three-carbon chain via Heck-coupling employing standard conditions. This gave ethyl cinnamate **22**, which was fully deprotected to give the cinnamic acid **23**. Reduction of the double bond employing hydrogen gas and platinum(II) oxide in methanol gave the methyl ester of **17**. The crude ester was saponified to give **17** in excellent yields including both steps. Considering the reduction of the double bond, the reaction is high yielding and no reduction of the chlorines could be observed during the course of reaction. Other combinations of catalysts, solvent, and hydrogen pressure, alternatively transfer hydrogenation, can be employed for reduction. But with more active catalysts such as palladium on carbon, with increased pressures of hydrogen and/or higher temperatures, there is an increased risk of dehalogenation.[27−29] The total yield using the described sequence above is 56%, and was again the preferred method for preparation of **17**.

Effects of the Ligands on Thyroid Hormone Receptors. The results of a radioligand binding assay for the human TRα_1 and TRβ_1, as well as a reporter cell assay employing CHOK1-cells (Chinese Hamster Ovary cells) stably transfected with hTRα_1 or hTRβ_1 and an alkaline phosphate reporter gene downstream thyroid response element (TRAFα_1 and TRAFβ_1), are summarized in Table 2. From the series of homologous carboxylic acid derivatives, increasing chain length was found to have a profound effect on affinity and selectivity. Affinity increases in the order formic (**11b**), acetic (**15**), and propionic acid (**17**), while β_1-selectivity is highest when the R_1-position is substituted with acetic acid. A similar structure−activity relationship is evident when the bromo homologues **6**, **7**, and **11a** are compared, but affinity is on average 10-fold higher when compared with the corresponding chloro analogues. The results from TRAFα_1 and β_1 reflect similar trends as the binding data, but with lower degree of for selectivity. All ligands display full agonism in the TRAF assay. On the basis of isoform selectivity, **11a** and **15** were selected for further studies in vivo.

Effects of the Ligands on a Cholesterol-Fed Rat Model. Dose−response data for **2**, **11a**, and **15** are shown in Table 3. The data are shown as ED_{15} for heart rate (dose causing 15% increase from vehicle), ED_{50} for cholesterol, and TSH suppression (dose causing 50% suppression from vehicle). Potency for tachycardia was significantly reduced for the TRβ_1 selective compounds, even when normalized for differences in potency. Nevertheless, both **11a** and **15** retained the cholesterol-lowering potency of **2**. The potency ratios clearly show the selectivity for these compounds by dividing the ED_{15} for heart rate/ED_{50} cholesterol. When normalized in this manner, both compounds are over 10-fold more selective than **2** for cholesterol-lowering versus tachycardia.

Table 3. Effects of the Ligands on a Cholesterol-Fed Rat Model[a]

compd	ED_{15} HR	ED_{50} chol	ED_{50} TSH	HR/chol	TSH/chol
2	14	20	7	0.7	0.3
11a	926	95.4	<46.2	9.7	<0.5
15	1077	82	38	13.1	0.4

[a] ED-values are expressed as nmol/kg/day. Administration was subcutaneous.

Crystal Structure of TRα and TRβ LBD in Complex with 15. In an effort to understand the structural basis for the β-selectivity of **15**, the structures of the ligand binding domains (LBD) of TRα_1 and TRβ_1, in complex with **15**, were determined to a resolution of 2.5 and 2.7 Å, respectively. The crystal structures discussed here were solved in crystal forms ($P6_522$ and $C222_1$ for TRα and TRβ, respectively) different from those published previously (C2 and $P3_12_1$ for TRα and TRβ, respectively).[6,12] The two receptor subtypes adopt a very similar α-helical structure with an rms difference of 0.63 Å calculated on the basis of the superimposition of 237 Cα atoms. The TRα_1 structure exhibits two flexible loops where no or only weak density is observed: the loop after helix 1 (180−186) and the loop before helix 3 (200−204). Due to differences in crystal packing, these loops are more ordered in TRβ_1. The hormone binding pocket, deeply buried within the receptor, differ only by one single amino acid residue, Asn331 in TRβ_1, which is substituted by Ser277 in TRα_1.

The mode of ligand binding is very similar in the two receptors, and an overlay of TRα_1 and TRβ_1 LBD is showed in Figure 2. As previously observed, His381α/His435β forms a hydrogen bond to the 4′-hydroxyl of the ligand.[6,12−13] Atom O4 of the ligand carboxylate hydrogen bonds to a water molecule, which is further bound to the main chain carbonyl oxygen atom of Ala 225α/279β and to the side chain of Arg262α/316β (NH1). Only in TRβ_1 can this water molecule also form an additional hydrogen bond to Arg282β (NH2). The second carboxylate oxygen, O3, forms a hydrogen bond to the main chain amide of Ser277α /Asn331β and to a water molecule. The water molecule is further bound to the main chain carbonyl of Thr275α/329β and the main chain amide of Gly278α/332β. In TRβ this water is also interacting with Arg320β. In TRα, the electron density for the analogous arginine (Arg266α) is less defined, and it is not possible to determine the exact position of the side chain or if a hydrogen bond to the water can be formed.

On the basis of the crystal structures, we conclude that the binding of **15** is very similar in the two receptors. The only significant difference between these two receptor complexes is a conformational change

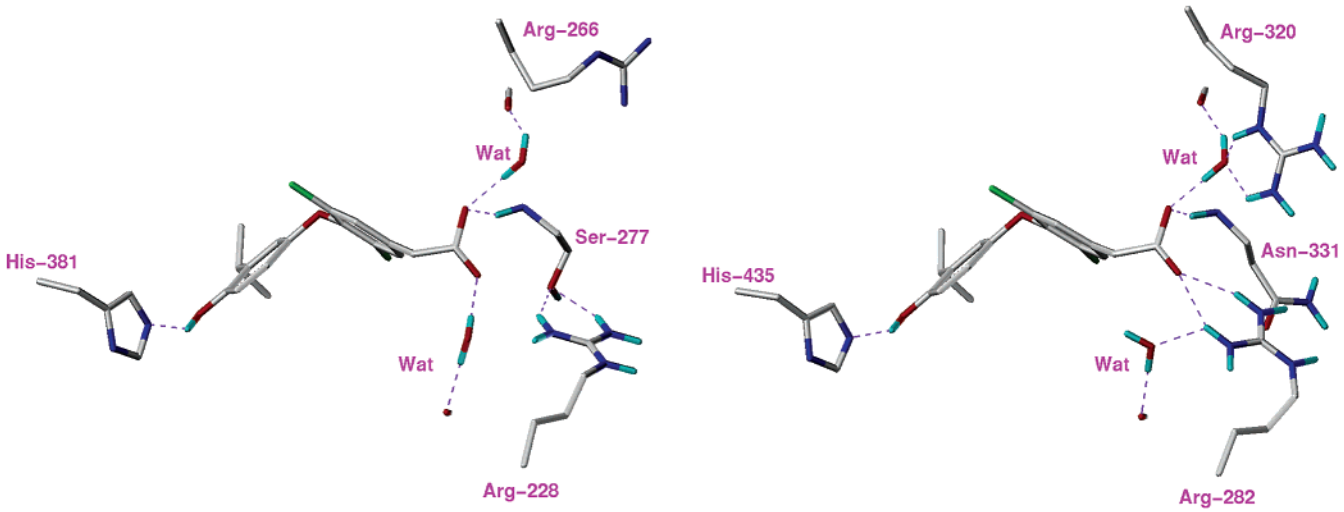

Figure 2. Interaction of the ligand **15** with TRα (left) and TRβ (right) as seen in the crystallographic structures of the LBD/ligand complexes (see text). Carbon atoms are depicted as white, oxygen as red, nitrogen as blue, chlorine as green, and hydrogen as cyan. Hydrogen bonding interactions are represented as dashed purple lines. In the TRα complex, Arg-228 forms two hydrogen bonds with Ser-277 while the corresponding Arg-282 in TRβ forms a bifurcated hydrogen bond to one of the carboxylate oxygen atoms of ligand **15**. The strong electrostatic interaction between the Arg-282 and the ligand accounts for the selectivity of this ligand for TRβ.

observed between Arg228α and 282β, which positions the terminal guanidino N-ω and -ω' atoms of Arg282β closer to the ligand carboxylate atom O4 (3.2 and 3.3 Å in TRβ vs 3.3 and 5.3 Å in TRα). This results in a significantly stronger electrostatic attraction between the ligand and the receptor in TRβ. The divergence in the conformation of Arg228α/282β between the two receptor isoforms is a direct consequence of the amino acid difference at Ser277α/Asn331β. In TRα, Arg228 is locked in the observed crystallographic orientation through the formation of two hydrogen bonds to Ser277, while in TRβ, the larger Asn331 side chain sterically repulses the corresponding Arg282 to a position that is much closer to the carboxylate group of the ligand. The net result of the Ser277α/Asn331β substitution is the replacement of two intramolecular hydrogen bonds between Ser277α and Arg228α with a bifurcated salt bridge between Arg282β and the ligand carboxylate atom O4. This bifurcated salt bridge probably accounts for the majority of the increased selectivity of **15** for TRβ. The importance of the interaction between Ser277α/Asn331β and Arg228α/282β regarding rat TRα_1 and human TRβ_1 in their binding to TRIAC has been discussed previously.[13] The conformational difference seen between Arg266α and 320β may also contribute for the higher affinity of **15** for TRβ, since the later side chain is positioned closer to the carboxylate group of the ligand. However, given this residue is further removed from the ligand and the electron density is very weak for this side chain in TRα_1 (probably due to it's location close to the flexible region after helix-1), the contribution of this residue to the selectivity is less certain.

Conclusions and Summary

On the basis of the data reported herein, a number of tentative conclusions can be drawn. Structural features determining β_1-selectivity for a TR-ligand largely depend on the length of the carboxylic acid side chain, and to a lesser degree on the halogen substituents at the R_3- and R_5-positions. The X-ray crystallographic structures of the LBD of TRα_1 and TRβ_1 in complex with **15** reveal that the single amino acid difference in the ligand binding pocket (Ser277 in TRα_1 or Asn331 in TRβ_1) results in a significantly different hydrogen bonding pattern that accounts for its β_1-selectivity. The in vitro potency of **11a** and **15** are in the same range as for **2**, which is reflected in vivo by cholesterol-lowering effects. On the other hand, potency for tachycardia is significantly reduced for **11a** and **15**, leaving an approximately 10-fold therapeutic window between heart rate and cholesterol lowering. Optimum combined properties of potent and selective action in vivo was found with **15**. Since all data presented here appears to be consistent with the action of ligands that are approximately 10-fold more selective for TRβ_1, it might be assumed that bioavailable ligands with larger β-selectivity would give an even larger therapeutic window in vivo. A similar pharmacological profile as **15** has been revealed previously with GC-1, but the preferred accumulation of GC-1 in the liver vs the heart probably also contributes to its marked lipid-lowering effect vs the absent effect on heart rate.[21] The effects of β_1-selective thyroid hormone receptor agonists should be further evaluated in relevant animal models and with additional measured parameters such as oxygen consumption and liver metabolism, prior to any clinical evaluation of its potential therapeutic properties.

Experimental Section

Chemistry. General Methods. All melting points were measured in open capillary tubes on a Gallenkamp Variable Heater and are uncorrected. Mikrokemi, Uppsala, Sweden, carried out the elemental analyses. NMR spectra were recorded on a JEOL-270 spectrometer. Coupling constants (J) are expressed in Hz and chemical shifts (δ) in ppm. Mass spectra were recorded on a Perkin-Elmer, API 150Ex spectrometer, with turbo "ion spray" in negative ion mode (ES-1) or positive (ES+1), using a Zorbax SB−C8 column (LC-MS). All solvents and reagents were purchased from commercial sources as analytical grade and used without further purification. When the compounds were purified by chromatography,

silica gel 60 (mesh) particle size was used (purchased from Merck Schucart).

3,5-Dibromo-4-(4-hydroxy-3-isopropylphenoxy)phenylacetic Acid (11a). To a suspension of bis(3-isopropyl-4-methoxyphenyl)iodonium tetrafluoroborate[23] (9.5 g) (**9**) and copper bronze (1.6 g) in dichloromethane (40 mL) was added a solution of methyl (3,5-dibromo-4-hydroxyphenyl)acetate (5 g) (**8a**) and triethylamine (1.4 g) in dichloromethane (25 mL) dropwise at room temperature. The mixture was stirred overnight and then filtered through Celite. Purification on a column (silica gel) and recrystallization from methanol gave 7.3 g (83%) of methyl [3,5-dibromo-4-(4-methoxy-3-isopropylphenoxy)phenyl] acetate (**10a**): ^{1}H NMR ($CDCl_3$) δ 1.18 (d, 6H, J = 6.9 Hz), 3.28 (m, 1H), 3.59 (s, 2H), 3.73 (s, 3H), 3.76 (s, 3H), 6.40 (dd, 1H, J = 8.7 Hz, J = 3.2 Hz), 6.68 (d, 1H, J = 8.9 Hz), 6.85 (d, 1H, J = 3.2 Hz), 7.52 (s, 2H); ^{13}C NMR ($CDCl_3$) δ 22.6, 27.1, 39.7, 52.5, 55.8, 110.8, 111.5, 114.3, 118.9, 133.4, 133.9, 138.8, 148.9, 150.7, 152.3, 170.9; LC-MS (ES-1), *m*/*z* 471 (M); LC-MS (ES+1), *m*/*z* 473 (M).

A mixture of **10a** (2.4 g) and boron tribromide (1 N in methylene chloride, 26 mL) in methylene chloride (100 mL) was stirred in methylene chloride at 0 °C. The reaction mixture was stirred for 16 h at room temperature before quenching with an ice and water mixture. The layers were separated, and the water layer was extracted with methylene chloride. The combined organic extracts were dried, filtered, and concentrated. The residue was purified on a column (silica gel, chloroform/methanol/acetic acid 95:5:0.5) to give 1.37 g (62%) of 3,5-dibromo-4-(4-hydroxy-3-isopropylphenoxy)phenylacetic acid **11a** as a white amorphous mass: mp 155−156 °C; ^{1}H NMR (methanol-d_4) δ 1.14 (d, 6H, J = 6.9 Hz), 3.22 (m, 1H), 3.62 (s, 2H), 6.40 (dd, 1H, J = 8.7 Hz, J = 3.2 Hz), 6.63 (d, 1H, J = 8.6 Hz), 6.65 (d, 1H, J = 2.5 Hz), 7.58 (s, 2H); ^{13}C NMR (methanol-d_4) δ 21.7, 26.9, 39.1, 111.9, 113.0, 115.1, 118.2, 133.9, 134.7, 136.2, 148.6, 149.3, 150.1, 173.3; LC-MS (ES-1), *m*/*z* 443 (M); LC-MS (ES+1), *m*/*z* 445 (M); Anal. Calcd for $C_{17}H_{16}Br_2O_4$: C, H, O.

3,5-Dichloro-4-(4-hydroxy-3-isopropylphenoxy)benzoic Acid (11b). Methyl 3,5-dichloro-4-hydroxybenzoate (10 g) (**8b**) was coupled with **9** (35 g) as described for the preparation of **10a**. Purification on column (silica gel, light petroleum ether/ethyl acetate 95:5) followed by recrystallization from methanol gave 8.42 g (51%) of methyl 3,5-dichloro-4-(4-methoxy-3-isopropylphenoxy)benzoate (**10b**): ^{1}H NMR (acetone-d_6) δ 1.15 (d, 6H, J = 6.9), 3.28 (m, 1H), 3.80 (s, 3H), 3.93 (s, 3H), 6.53 (dd, 1H, J = 8.7, J = 3.22), 6.84 (d, 1H, J = 2.7), 6.86 (d, 1H, J = 6.2), 8.07 (s, 2H); ^{13}C NMR (methanol-d_4) δ 21.9, 26.8, 52.3, 55.4, 111.4, 111.9, 113.6, 128.9, 130.0, 130.4, 138.5, 150.6, 151.3, 152.7, 164.0.

A mixture of **10b** (100 mg), NaOH (1 N, 1 mL), and methanol (2.5 mL) was stirred at room temperature. When the starting material was consumed, the reaction mixture was concentrated, the residue neutralized with HCl, and the aqueous phase extracted with ethyl acetate. Concentration in vacuo of the reaction mixture gave the intermediate 3,5-dichloro-4-(4-methoxy-3-isopropyl-phenoxy)benzoic acid which was used in the next step without further purification. The intermediate methoxy compound was deprotected using the method as described for the preparation of **11a** to give 65 mg (71%) of 3,5-dichloro-4-(4-hydroxy-3-isopropylphenoxy)benzoic acid: mp 182−184 °C; ^{1}H NMR (acetone-d_6) δ 1.18 (d, 6H, J = 6.9 Hz), 3.29 (m, 1H), 6.42 (dd, 1H, J = 8.6 Hz, J = 3.0 Hz), 6.76 (d, 1H, J = 8.9 Hz), 6.80 (d, 1H, J = 3.2 Hz), 8.08 (s, 2H); ^{13}C NMR (acetone-d_6) δ 21.9, 27.1, 112.2, 113.5, 115.4, 129.0, 130.0, 130.6, 136.3, 150.0, 150.1, 151.4, 164.1; LC-MS (ES-1), *m*/*z* 339 (M). Anal. Calcd for $C_{16}H_{14}Cl_2O_4$: C, 56.3; H, 4.1; O, 18.8. Found: C, 55.3; H, 4.3; O, 18.4.

3,5-Dichloro-4-(4-hydroxy-3-isopropylphenoxy)phenylacetic Acid (15). Method A. Methyl 3,5-dichloro-4-(4-methoxy-3-isopropylphenoxy)benzoate (**10a**) (3.0 g, 8.4 mmol) was treated with diisobutyl aluminum hydride (1 N, 25 mL) in THF (32 mL) at 0 °C and then warmed to room temperature and stirred overnight. The reaction mixture was poured into ice-cold aqueous HCl (1 N) and extracted three times with ethyl acetate. The organic layer was washed with brine, dried over $MgSO_4$, and concentrated to give 3.20 g (quantitative yield) of 3,5-dichloro-4-(4-methoxy-3-isopropylphenoxy)benzyl alcohol (**12**) as an oil: ^{1}H NMR (acetone-d_6) δ 1.15 (d, 6H, J = 6.9 Hz), 3.27 (m, 1H), 3.79 (s, 3H), 4.69 (s, 2H), 6.46 (dd, 1H, J = 8.9 Hz, J = 3.0 Hz), 6.81 (d, 1H, J = 3.2 Hz), 6.84 (d, 1H, J = 8.9 Hz), 7.5 (s, 2H); ^{13}C NMR (acetone-d_6) δ 22.0, 26.8, 55.4, 62.2, 111.3, 111.6, 127.1, 129.3, 138.3, 142.1, 145.9, 151.1, 152.4; LC-MS (ES+1), *m*/*z* 342 (M).

The alcohol **12** (3.21 g) was added into a mixture of P_2O_5 (0.58 g) and H_3PO_4 (5.5 mL) followed by addition of sodium iodide (2.43 g). The reaction mixture was stirred at 120 °C for 15 min and then partitioned between water and ethyl acetate. The organic layer was washed with $Na_2S_2O_3$ (saturated) and brine, dried over $MgSO_4$, and concentrated. The residue was recrystallized from petroleum ether to give 2.9 g (79%) of 3,5-dichloro-4-(4-methoxy-3-isopropyl-phenoxy)benzyl iodide (**13**): ^{1}H NMR ($CDCl_3$) δ 1.16 (d, 6H, J = 6.9 Hz), 3.27 (m, 1H), 3.76 (s, 3H), 4.35 (s, 2H), 6.40 (dd, 1H, J = 8.9 Hz, J = 3.0 Hz), 6.67 (d, 1H, J = 8.9 Hz), 6.84 (d, 1H, J = 3.2 Hz), 7.37 (s, 2H); ^{13}C NMR ($CDCl_3$) δ 22.6, 27.0, 31.0, 55.9, 110.8, 111.4, 114.1, 129.4, 130.1, 137.8, 138.9, 147.3, 150.8, 152.4.

To a solution of sodium cyanide (400 mg) in water (1.0 mL) was added the above iodide **13** (900 mg) in absolute ethanol (3 mL). The reaction mixture became homogeneous after heating and was stirred under reflux for 2 h. The reaction mixture was poured into crushed ice and partitioned between water and ethyl acetate. The organic layer was dried, filtered, and concentrated, and the residue was chromatographed on silica gel and eluted with ethyl acetate/petroleum ether (1/8). The pure fractions were pooled and concentrated to give 440 mg (63%) 3,5-dichloro-4-(4-methoxy-3-isopropylphenoxy)phenylacetonitrile. The intermediate methoxy compound (170 mg) was deprotected using the method as described for the preparation of **11a** to give 147 mg (90%) of 3,5-dichloro-4-(4-hydroxy-3-isopropylphenoxy)phenylacetonitrile (**14**): mp 136−137 °C ^{1}H NMR (acetone-d_6) δ 1.17 (d, 6H, J = 6.9 Hz), 3.28 (m, 1H), 4.97 (s, 2H), 6.36 (dd, 1H, J = 8.7 Hz, J = 3.2 Hz); 6.74 (d, 1H, J = 8.7 Hz), 6.77 (d, 1H, J = 3.0 Hz), 7.60 (s, 2H); 8.04 (s, 1H); ^{13}C NMR (acetone-d_6) δ 21.9, 27.1, 70.0, 112.0, 113.3, 115.5, 117.5, 129.3, 130.0, 130.7, 136.3, 147.3, 149.9, 150.3; LC-MS (ES-1), *m*/*z* 334 (M).

To a solution of **14** (760 mg) dissolved in acetic acid (10 mL) was added dropwise a mixture of concentrated sulfuric acid (10 mL) and water (10 mL). The reaction mixture was heated at 105 °C for 3 h and partitioned between ice-cold water and ethyl acetate. The organic layer was dried, filtered, and concentrated to give 638 mg (77%) of 3,5-dichloro-4-(4-hydroxy-3-isopropyl-phenoxy)phenylacetic acid (**15**): mp 132−134 °C;^{1}H NMR (acetone-d_6) δ 1.18 (d, 6H, J = 6.9 Hz), 3.28 (m, 1H), 3.74 (s, 2H), 6.34 (dd, 1H, J = 8.7 Hz, J = 3.2 Hz), 6.73 (d, 1H, J = 8.7 Hz), 6.77 (d, 1H, J = 3.0 Hz), 7.51 (s, 2H); ^{13}C NMR (acetone-d_6) δ 21.9, 27.1, 38.8, 111.8, 113.3, 115.4, 129.2, 130.6, 134.3, 136.2, 146.4, 149.7, 150.4, 171.1; LC-MS (ES-1), *m*/*z* 353 (M); Anal. ($C_{17}H_{16}Cl_2O_4$) C, H, O.

Method B. 4-Bromo-3,5-dichlorophenol (1.84 g, 7.6 mmol) was coupled with bis(3-isopropyl-4-methoxyphenyl)iodonium tetrafluoroborate, as described for the preparation of **10a**. Purification on column (silica gel, light petroleum ether/ethyl acetate 95:5) gave 2.0 g (70%) of 3,5-dichloro-4-(4-methoxy-3-isopropylphenoxy)phenyl bromide (**19**): ^{1}H NMR ($CDCl_3$) δ 1.17 (d, J = 6.9 Hz, 6H), 3.27 (m, 1H), 3.77 (s, 3H), 6.42 (dd, J = 3.2 Hz, J = 8.9 Hz, 1H), 6.69 (d, J = 8.9 Hz, 1H), 6.82 (J = 3.2 Hz, 1H), 7.55 (s, 2H); ^{13}C NMR ($CDCl_3$) δ 22.6, 27.0, 55.9, 110.9, 111.4, 114.0, 117.6, 131.1, 131.9, 138.9, 147.4, 150.6, 152.5.

An mixture of **19** (2.0 g, 5.0 mmol), trimethylsilylacetylene (0.6 g, 6.0 mmol), $PdCl_2(PPh_3)_2$ (0.18 g, 0.25 mmol), CuI (0.16 mg), and triethylamine (1.0 g) in DMF (20 mL) was heated at 100 °C for 4 h. After concentration in vacuo, the residue was taken up in ethyl acetate and washed with HCl (1 N). The organic phase was further washed with $NaHCO_3$ (aq) and NaCl (aq) and dried over $MgSO_4$. After concentration, the residue was subjected to column chromatography (silica gel,

petroleum ether/ethyl acetate 98:2) to give 1.5 g (74%) of 3,5-dichloro-4-(4-hydroxy-3-isopropylphenoxy)phenyltrimethylsilylacetylene: ^{1}H NMR ($CDCl_3$) δ 0.23 (s, 9H), 1.13 (d, J = 6.93 Hz, 6H), 3.26 (m, 1H), 3.77 (s, 3H), 6.44 (dd, J = 3.2 Hz, J = 8.9, 1H), 6.69 (d, J = 8.9, 1H); 6.80 (d, J = 3.2, 1H), 7.48 (m, 2H); ^{13}C NMR ($CDCl_3$) δ −0.2, 22.6, 27.0, 55.9, 97.0, 101.0, 110.9, 111.6, 113.9, 121.5, 130.0, 132.4, 138.9, 148, 150.8, 152.4; LC-MS.

Cyclohexene (0.90 g, 11 mmol) was added a solution of BH_3−THF complex in THF (1 N) and stirred for 30 min, compound **20** (600 mg, 1.6 mmol) in THF (10 mL) was added, and the reaction was stirred for 2 h. Then a mixture of NaOH (1 N, 4 mL) and MeOH (6 mL) was added to the reaction mixture, followed by H_2O_2 (30%, 2 mL). The reaction mixture was stirred for 1 h after the last addition. The temperature in the flask was kept at 0 °C through all the above additions, which were also conducted dropwise. After concentration in vacuo, the residue was taken up in ethyl acetate, washed with HCl (2 N), and dried over $MgSO_4$. After concentration, the residue was subjected to column chromatography (silica gel, chlorform/methanol 95:5) to give 0.35 g (59%) of 3,5-dichloro-4-(4-methoxy-3-isopropylphenoxy)phenylacetic acid (**21**): ^{1}H NMR ($CDCl_3$) δ 1.16 (d, J = 6.93 Hz, 6H), 3.25 (m, 1H), 3.59 (s, 2H), 3.69 (s, 3H), 6.39 (dd, J = 3.0 Hz, J = 8.9 Hz, 1H), 6.65 (d, J = 8.9 Hz), 6.86 (d, J = 3.0 Hz), 7.30 (s, 2H); ^{13}C NMR ($CDCl_3$) δ 22.6, 27.0, 40.0, 55.90, 110.8, 111.3, 114.2, 130.1, 130.1, 132.0, 138.8, 147.0, 150.9, 152.3.

The intermediate methoxy compound **21** (0.35 g) was deprotected using the method described for the preparation of **11a** to give 0.31 g (93%) of **15**.

3,5-Dichloro-4-(4-hydroxy-3-isopropylphenoxy)phenylpropionic Acid (17). Method A. Sodium (0.046 g) in small pieces was added into a dry flask containing *tert*-butyl alcohol. The mixture was refluxed for 1 h or until the sodium was completely dissolved. Ethyl malonate (0.32 g) was added, and the reaction mixture was heated at 90 °C for 1 h followed by addition of **13** (0.45 g) in portions. The mixture was stirred under reflux for 3 h and concentrated. The residue was stirred under reflux with potassium hydroxide and water (1:1) overnight. The resulting residue was partitioned between ethyl acetate and concentrated HCl (1 N). The organic layer was dried, filtered, and concentrated to give a solid, which was transferred into a small flask, which was heated at 180 °C for 3 h. The residue was purified on column (silica gel, chloroform/methanol/acetic acid 98:3:0.3). This gave 0.15 g (20%) of 3,5-dichloro-4-(4-methoxy-3-isopropylphenoxy)phenylpropionic acid (**16**) as a pale yellow mass: ^{1}H NMR (methanol-d_4) δ 1.14 (d, 6H, J = 6.9 Hz), 2.64 (t, 2H, J = 7.4), 2.92 (t, 2H, J = 7.4), 3.29 (m, 1H), 3.76 (s, 3H), 4.69 (s, 2H), 6.41 (dd, 1H, J = 8.9 Hz, J = 3.2 Hz), 6.71 (d, 1H, J = 3.2 Hz), 6.78 (d, 1H, J = 8.9 Hz), 7.36 (s, 2H); ^{13}C NMR (methanol-d_4) δ 21.6, 26.7, 29.6, 34.7, 55.0, 111.0, 111.4, 113.0, 129.0, 129.4, 138.2, 140.2, 145.8, 151.1, 152.3, 174.7; LC-MS (ES-1), m/z 381 (M).

Boron trifluoride−dimethyl sulfide (1.0 mL) was added to a well-stirred solution of **16** (120 mg) in dichloromethane (10 mL). The resulting reaction mixture was stirred at room temperature for 18 h and then treated with water. The organic phase was separated and the aqueous phase extracted with dichloromethane. The combined organic extracts were concentrated, and the residue was recrystallized from dichloromethane and light petroleum ether to give 33 mg (30%) of 3,5-dichloro-4-(4-hydroxy-3-isopropylphenoxy)phenylpropionic acid: ^{1}H NMR (methanol-d_4) δ 1.14 (d, 6H, J = 6.9), 2.64 (t, 2H, J = 7.2), 2.92 (t, 2H, J = 7.2), 6.30 (dd, 1H, J = 8.7, J = 3.0), 6.61 (d, 1H, J = 8.4), 6.63 (d, 1H, J = 3.0), 7.35 (s, 2H); ^{13}C NMR (methanol-d_4) δ 21.5, 26.8, 29.6, 43.8, 11.7, 112.7, 115.0, 129.0, 129.4, 136.1, 140.1, 145.9, 149.4, 150.4, 152.0, 174.8; LC-MS (ES-1), m/z 367, 369 (M); Anal. ($C_{18}H_{18}Cl_2O_4$) C, H, O.

Method B. A mixture of **19** (1.3 g, 3.3 mmol), ethyl acrylate (0.40 g, 4.0 mmol), palladium acetate (0.080 mg, 0.30 mmol), triphenylphosphine (0.082 g, 0.33 mmol), triethylamine (1.0 mL), and dimethylformamide (25 mL) was stirred at 100 °C for 48 h. The reaction mixture was concentrated and the residue taken up in ethyl acetate. The organic phase was washed with hydrochloric acid (1 N), followed by sodium bicarbonate (aqueous, saturated solution). The organic phase was concentrated and recrystallized from petroleum ether/diethyl ether, to give 1.28 g (95%) of methyl 3,5-dichloro-4-(4-hydroxy-3-isopropylphenoxy)cinnamate (**22**): ^{1}H NMR (acetone-d_6) δ 1.16 (d, 6H, J = 6.9), 1.29 (t, 3H, J = 6.93), 3.28 (m 1H), 3.79 (s, 3H), 4.23 (dd, 2H, J = 7.2), 6.51 (dd, 1H, J = 8.9, J = 3.0), 6.70 (d, 1H, J = 16), 6.85 (d, 1H, J = 8.7), 6.86 (d, 1H, J = 3.0), 7.65 (d, 1H, J = 16), 7.92 (s, 2H); ^{13}C NMR (acetone-d_6) δ 13.8, 22.0, 26.8, 55.4, 60.3, 111.4, 111.8, 113.5, 121.1, 129.0, 130.2, 133.8, 138.4, 140.9, 148.5, 150.9, 152.6, 165.7; LC-MS (ES-1), m/z 365, 367 (M).

The methoxy cinnamic ester **22** was demethylated and subsequently saponified according to the procedures as described for the preparation of **17** and **10b**. The yield for the two steps was quantitative. The analytical sample was recrystallized from ethyl acetate/petroleum ether to give 3,5-dichloro-4-(4-hydroxy-3-isopropylphenoxy)cinnamic acid (**23**): ^{1}H NMR (methanol-d_4) δ 1.15 (d, 6H, J = 6.9 Hz), 3.23 (m, 1H), 6.35 (dd, 1H, J = 8.7 Hz, J = 3.1 Hz), 6.63 (d, 1H, J = 8.7 Hz), 6.6−6.68 (1H, peaks and coupling constant obscured by the doublets at 6.63 and 6.66), 6.66 (d, 1H, J = 3.1); 7.59 (d, 1H, J = 15.8 Hz); 7.74 (s, 2H); ^{13}C NMR (methanol-d_4) δ 21.5, 26.9, 128.5, 130.3, 136.3, 148.8, 149.7, 150.2, 151.3, 151.7, 152.1, 152.3, 152.6, 153.0, 153.3; LC-MS (ES-1), m/z 365, 367 (M).

3,5-Dichloro-4-(4′-hydroxy-3′-isopropylphenoxy)cinnamic acid (20 mg) was dissolved in methanol (3 mL). The solution was hydrogenated under atmospheric pressure over PtO_2 (5 mg) with stirring for 6 h. The catalyst was removed by filtration (Celite), and the filtrate was concentrated under vacuum. The resulting residue was dissolved in NaOH (1 N, 3 mL) and methanol (3 mL). The reaction mixture was stirred at room temperature for 4 h. The organic phase was removed under vacuum, and the aqueous solution was acidified with HCl (1 N). The water phase was extracted with ethyl acetate (3 × 15 mL), and the combined organic phase was washed with brine, dried ($MgSO_4$), filtered, and concentrated. The residue was crystallized from ether/*n*-heptane to give 17 mg (84%) of 3,5-dichloro-4-(4-hydroxy-3-isopropylphenoxy)phenylpropionic acid (**17**) as a solid.

ThR-Binding Assay. This assay has been described in detail previously.[30,31] The concentration of each compound required to inhibit 50% of binding of ^{125}I−T_3 to hTR$_1$ (IC_{50}) is presented in Tables 1 and 2, respectively. The competition binding experiments were evaluated by a nonlinear four-parameter logistic model: $b = ((b_{max} - b_{min})/(1 + (I/IC_{50})^S)) + b_{min}$. Where b_{max} is the total concentration of binding sites, b_{min} is the nonspecific binding, I is the added concentration of binding inhibitor, IC_{50} is the concentration of binding inhibitor at half-maximal binding, and S is a slope factor.[32] The K_d for the tracer (125[I]-T_3) is lower for hTHRα_1 (58 ± 5 pM) than for hTHRβ_1 (112 ± 8 pM), and as a consequence the IC_{50} value for an unlabeled compound with equal affinity (K_i) for the two subtypes will be lower for hTHRβ_1 than for hTHRα_1. The Cheng−Prusoff relationship for a competitive inhibitor is used to obtain the affinity (K_i) for a compound to the hTRs: $K_i = IC_{50}/(1 + L/K_d)$ where L = free concentration of the tracer and $K_d = K_d$ for tracer; K_i: hTHRα_1 = $IC_{50}/(1 + 200/58) = IC_{50}/4.45$. K_i: hTHRβ_1 = $IC_{50}/(1+200/112) = IC_{50}/2.79$. hTR-receptor selectivity is therefore calculated as IC_{50} (hTHRα_1)/IC_{50} (hTHRβ_1) × 1.7.

Vector Constructs, Generation of Reporter Cell Lines (TRAF), and Assay Procedure. The cDNAs encoding the full length human THRα_1 and THRβ_1 were cloned in the mammalian expression vector pMT-hGH.[33−35] The pDR4-ALP reporter vector contains one copy of the direct repeat sequence AGGTCA nnnnAGGTCA, fused upstream of the core promoter sequences of the mouse mammary tumor virus long terminal repeat (MMTV), replacing the glucocorticoid response elements. The DR4-MMTV promoter fragment was then cloned in the 5′ end of the cDNA encoding human placental alkaline phosphatase (ALP),[36] followed in the 3′-end by the polyA-signal sequence of the human growth hormone gene.[35] Chinese

hamster ovary (CHO) K1 cells (ATCC No. CCL 61) were transfected in two steps, first with the receptor expression vectors pMT-hThRα_1 and pMT-ThRβ_1, respectively, and the drug resistance vector pSV2−Neo,[37] and in the second step, with the reporter vector pDR4-ALP and the drug resistance vector p*K*SV−Hyg.[38] Individual drug resistant clones were isolated and selected based on T_3 inducibility. One stable reporter cell clone each of CHO/hThRα_1 and CHO/hTHRβ_1 were chosen for further study in response to various thyroid hormone agonists. The procedure for characterization of agonism/antagonism of ligands has previously been described in detail.[34] Toxicity was assessed by microscopic evaluation of cell morphology and by the MTS/PMS assay (CellTiter 96 Cell Proliferation Assay), in which the mitochondrial formation of a colored tetrazolium salt is measured spectrophotometrically at 492 nm (Promega Corporation, technical Bulletin No 169). The absorbance is directly proportional to the number of living cells in culture.

In Vivo Effects of 2, 11a, and 15 in Cholesterol-Fed Rats after Subcutaneous Administration. Effects in vivo were determined using male Sprague−Dawley rats. They were fed standard chow supplemented with cholesterol (1.5%) and cholic acid (0.5%), and this was continued for 2 weeks in order to achieve total cholesterol levels of approximately 200 mg/dL. After this, animals were injected subcutaneously (s.c.) with vehicle (10% *m*-pyrol, 5% ethanol, 5% cremaphor, 80% water, $n = 6$), increasing doses of **2** ($n = 6$/dose), **11a** ($n = 6$/dose), or **15** ($n = 6$/dose) once per day for 7 days. **2** was administered in dose increments from 1.54 nmol/kg/day to 924 nmol/kg/day. Both **11a** and **15** were dosed incrementally between 15.4 and 9240 nmol/kg/day, also for 7 days. After 7 days treatment, the rats were anesthetized using 30 mg/kg pentobarbital (Abbott Labs, Chicago, IL), and heart rate was determined using lead II ECG (Gould recorders, Valley View, OH). Blood was then withdrawn through the abdominal aorta for TSH and cholesterol determination. Plasma TSH levels were determined using an Amersham Rat RIA kit (Piscataway, NJ). Plasma cholesterol levels were determined using a Cobas-Mira analyzer (Roche Diagnostics, Somerville, NJ).

Protein Expression. Human TRα-LBD (6 x His E148-V410) and human TRβ-LBD (6 xHis G209-D461) were overexpressed in *Escherichia coli* BL21 (DE3) cells using the pET28a expression system. Fermentation was carried out in batch culture (2 × LB medium, 22 °C), and expression of the recombinant protein was induced by the addition of isopropyl β-D-thiogalactoside (IPTG) (0.55 mM) at $OD_{600} = 5.0$. After 4 h of induction, the cells were harvested by centrifugation. The cell pellet was resuspended and washed once with buffer (Hepes pH 8.0 (20 mM), KCl (100 mM), glycerol (10%), and monothioglycerol (MTG) (2.5 mM)). The final cell pellet was frozen at −70 °C.

Protein Purification. Cell pellet was thawed at room temperature and disrupted in a bead mill using lysis buffer (Hepes pH 8.0 (20 mM), glycerol (10%), MTG (2.5 mM), and phenylmethylsulfonyl fluoride (PMSF) (0.1 mM)). Lysate (corresponding to 1.8 L cells) was centrifuged, and the supernatant was applied to Talon resin (CLONTECH Laboratories, Inc., Palo Alto, CA). For TRβ, 2−5-fold molar excess of **15** was added to the extract before loading to the Talon column. Talon resin (40 mL) was packed in a XK26 column (Amersham Pharmacia Biotech, Sweden) and equilibrated with a mixture of imidazole (2.5 mM), Hepes pH 8.0 (20 mM), glycerol (10%), MTG (2.5 mM), and PMSF (0.1 mM). Bound protein was eluted with a mixture of imidazole (100 mM), Hepes pH 8.0 (20 mM), glycerol (10%), and MTG (2.5 mM). The His-tag of TRβ-LBD was thrombin cleaved by 10 U/mg on ice for 6−10 h. Pooled fractions were adjusted to 0.6 M ammonium sulfate and further purified by hydrophobic interaction chromatography (HIC) using Phenyl Sepharose FF low sub (Amersham Pharmacia Biotech, Sweden) as resin. The column (50 mL resin in XK26 column, Amersham Pharmacia Biotech, Sweden) was equilibrated with a mixture of Hepes pH 8.0 (20 mM), ammonium sulfate (600 mM), ethylenediaminetetraacetic acid (EDTA) (0.5 mM), and bound protein was, after washing, eluted with a 200 mL gradient from 600 mM salt to no salt (including 10% acetonitrile, 10% glycerol). Fractions were analyzed on SDS−PAGE and Native-PAGE (Phast System, Amersham Pharmacia Biotech, Sweden) and then pooled followed by concentration and buffer exchange (Hepes pH 8.0 (20 mM) and dithiothreitol (DTT) (3 mM)) using Centricon 30 (Millipore). Protein was frozen in aliquots at −70 °C.

Crystallization, X-ray Data Collection, and Structure Determination of TRα_1−LBD. The TRα_1−LBD ligand complex was crystallized, at room temperature, using hanging drop vapor diffusion from a drop (1 μL protein solution at 20 mg/mL, 1 μL of precipitant solution) suspended from a reservoir composed of ammonium sulfate (0.15 M), sodium citrate (pH 5.6, 0.03 M), and lithium sulfate (0.3 M). The purified TRα_1−LBD was incubated at 2 molar excess for 1.5 h on ice with **15**, prior to crystal setting. Hexagonal crystals appeared after 1 day and continued to grow for a couple of days. 2.5 Å diffraction data of TRα_1−LBD+**15** was collected at beam line ×13, DESY, Hamburg using a MARCCD detector. A single crystal was stepwise soaked in reservoir solution supplemented with increasing concentration of glycerol (final concentration of 30%), flash cooled in the home laboratory and transported to DESY in a liquid nitrogen dewar. Data were collected at 100 K using a wavelength of 0.8013 Å. Data processing was carried out with the HKL suite.[39] The TRα−**15** cocrystals belong to space group $P6_522$ with cell dimensions $a = b = 109.3$ Å, $c = 135.7$ Å, containing one molecule per asymmetric unit.

Crystallization, X-ray Data Collection, and Structure Determination of TRβ_1−LBD. The TR-LBD ligand complex was crystallized, at room temperature, using hanging drop vapor diffusion from a drop (1 μL protein solution at 20 mg/mL, 1 μL of precipitant solution) suspended from a reservoir composed of ammonium sulfate (1.95 M), Tris-HCl (pH 8.0, 0.1 M), and 3-(1-pyridino)-1-propanesulfonate (NDSB-201) (50 mM). The TRβ-**15** crystals were cryoprotected by crystallization solution containing glycerol (30%). Data were collected at 100 K using a rotating anode (Rigaku Ru300) equipped with OSMIC mirrors and a MAR345 detector. The TRβ_1−**15** cocrystals belong to the space group $C222_1$ with cell dimensions $a = 76.52$, $b = 107.74$, $c = 66.90$ Å. Indexing and integration of the TRβ_1 complex was done with the program MOSFLM[40] and scaled in SCALA.[41]

Refinement of TRα_1−LBD+15 and TRβ_1−LBD+15. Starting models for the refinement of the TRα_1 and TRβ_1 structures were TR complexes previously solved. In both cases, refinement was initiated with a round of rigid body refinement followed by simulated annealing starting at 2000 K. Well-defined electron density was observed in the ligand binding clefts in which **15** was built. Refinement and map calculations were performed with CNX.[42] All model building was done with the program "O".[43] The quality of the model was validated with the program PROCHECK.[42] Statistics from data collection and refinement are provided in Supporting Information. The figure of the ligand binding pocket was produced with Molscript[45] and rendered with Raster3D.[46]

Acknowledgment. The authors would like to thank Dr. Denis Ryono for valuable scientific as well as linguistic contributions to this manuscript, and Christian Betzel and Markus Perbandt for help with X-ray data collection.

Supporting Information Available: Table of statistics from data collection and refinement. This material is available free of charge via the Internet at http://pubs.acs.org.

References

(1) Lazar, M. A. Thyroid hormone receptors: Multiple forms, multiple possibilities. *Endocr. Rev.* **1993**, *14*, 184−193.
(2) Wikström, L.; Johansson, C.; Salto, C.; Barlow, C.; Campos Barros, A.; Baas, F.; Forrest, D.; Thoren, P., Vennström, B. Abnormal heart rate and body temperature in mice lacking thyroid hormone receptor a1. *EMBO J.* **1988**, *17*, 455−461.
(3) Johansson, C.; Vennström, B.; Thoren, P. Evidence that decreased heart rate in thyroid hormone receptor-a1-deficient mice is an intrinsic defect. *Am. J. Physiol.* **1998**, *275*, R640−R646.

(4) Forrest, D.; Vennström, B. Functions of thyroid hormone receptors in mice. *Thyroid* **2000**, *10*, 41−52.
(5) Takeda, K.; Sakurai, A.; DeGroot, L. J.; Refetoff, S. Recessive inheritance of thyroid hormone resistance caused by complete deletion of the protein-coding region of the thyroid hormone receptor-β gene. *J. Clin. Endocrin., Metab.* **1992**, *74*, 49−55.
(6) Wagner, R. L.; Apriletti, J. W.; McGrath, M. E.; West, B. L.; Baxter, J. D.; Fletterick, R. J. A structural role for hormone in the thyroid hormone receptor. *Nature* **1995**, *378*, 690−697.
(7) Bourguet, W.; Ruff, M.; Chambon, P.; Gronemeyer, H.; Moras, D. Crystal structure of the ligand-binding domain of the human nuclear receptor RXR-α. *Nature* **1995**, *375*, 377−382.
(8) Brzozowski, A. M.; Pike, P. D.; Dauter, Z.; Hubbard, R. E.; Bonn, T.; Engström, O.; Ohmna., L.; Green, G. L.; Gustafsson, J.-A.; Carlquist, M. Molecular basis of agonism and antagonism in the oestrogen receptor. *Nature* **1997**, *389*, 753−758.
(9) Renaud, J. P.; Rochel, N.; Ruff, M.; Vivat, V.; Chambon, P.; Gronemeyer, H.; Moras, D. Crystal structure of the RAR-γ ligand-binding domain bound to all-trans retinoic acid. *Nature* **1995**, *378*, 681−689.
(10) Xu, H. E.; Lambert, M. H.; Montana, V. G.; Parks, D. J.; Blanchard, S. G.; Brown, P. J.; Sternbach, D. D.; Lehmann, J. M.; Wisely, G. B.; Willson, T. M.; Kliewer, S. A.; Milburn, M. V. Molecular recognition of fatty acids by peroxisome proliferator-activated receptors. *Mol. Cell* **1999**, *3*, 397−403.
(11) Bledsoe, R. K.; Montana, V. G.; Stanley, T. B.; Delves, C. J.; Apolito, C. J.; McKee, D. D.; Consler, T. G.; Parks, D. J.; Stewart, E. L.; Willson, T. M.; Lambert, M. H.; Moore, J. T.; Pearce, K. H.; Xu, H. E. Crystal structure of the glucocorticoid receptor ligand binding domain reveals a novel mode of receptor dimerization and coactivator recognition. *Cell* **2002**, *110*, 93−105.
(12) Darimont, B. D.; Wagner, R. L.; Apriletti, J. W.; Stallcup, M. R.; Kushner, P. J.; Baxter, J. D.; Fletterick, R. J.; Yamamoto, K. R. Structure and specificity of nuclear receptor-coactivator interactions. *Genes Devel.* **1998**, *12*, 3343−3356.
(13) Wagner, R. L.; Huber, R. B.; Shiau, A. K.; Kelly, A.; Cunha Lima, S. T.; Scanlan, T. S.; Apriletti, J. W.; Baxter, J. D.; West, B. L.; Fletterick, R. J. Hormone selectivity in thyroid hormone receptors. *Mol. Endocrinol.* **2001**, *15*, 398−410.
(14) Loireau, A.; Autissier, N.; Dumas, P.; Michael, O.; Jorgensen, E. C.; Michael, R. Comparative effects of 3,5-dimethyl-3′isopropyl-L-thyronine (DIMIT) and 3,5-diiodo-3′-isopropylthyroacetic acid (IpTA2) on body weight gain and lipid metabolism in genetically obese Zucker rats. *Biochem. Pharmacol.* **1986**, *35*, 1691−1696.
(15) Engelken, S. F.; Eaton, R. P. The effects of altered thyroid status on lipid metabolism in the genetic hyperlipemic Zucker rat. *Atherosclerosis* **1981**, *38*, 177−188.
(16) Hansson, P.; Valdemarsson, S.; Nilsson-Ehle, P. Experimental hyperthyroidism in man: Effects on plasma lipoproteins, lipoprotein lipase and hepatic lipase. *Horm. Metab. Res.* **1983**, *15*, 449−452.
(17) Scarabottolo, L.; Trezzi, E.; Roma, P.; Catapano, A. L. Experimental hypothyroidism modulates the expression of low-density lipoprotein receptor by the liver. *Atherosclerosis* **1986**, *59*, 329−333.
(18) Jorgensen, E. C. Thyroid hormones and analogues. II. Structure−activity relationships. *Hormonal Proteins and Peptides*; Li, C. H., Ed.; Academic Press: New York: 1978; Vol. 6, pp 107−204.
(19) Dietrich, S. W.; Bolger, M. B.; Kollman, P. A.; Jorgensen, E. C. Thyroxine analogues. 23. Quantitative structure−activity correlation studies of an in vivo and in vitro thyromimetic activities. *J. Med. Chem.* **1977**, *20*, 863−880.
(20) Chiellini, G.; Apriletti, J. W.; Yoshihara, H. A.; Baxter, J. D.; Ribeiro, R. C. J.; Scanlan, T. S. A high-affinity subtype-selective agonist ligand for the thyroid hormone receptor. *Chem. Biol.* **1998**, *5*, 299−306.
(21) Trost, S. U.; Swanson, E.; Gloss, B.; Wang-Iverson, D. B.; Zhang, H.; Volodarsky, T.; Grover, G. J.; Baxter, J. D.; Chiellini, G.; Scanlan, T. S.; Dillmann, W. H. The thyroid hormone receptor-*b*-selective agonist GC-1 differentially affects plasma lipids and cardiac activity. *Endocrinology* **2000**, *141*, 3057−3064.
(22) Beck-Peccoz, P.; Sartorio, A.; De Medici, C.; Grugni, G.; Morabito, F.; Faglia, G. Dissociated thyromimetic effects of 3,5,3′-triiodothyroacetic acid (TRIAC) at the pituitary and peripheral tissue levels. *J. Endocrinol. Invest.* **1988**, *11*, 113−118.
(23) Yokoyama, N.; Walker, G. N.; Main, A. J.; Stanton, J. L.; Morrissey, M. M.; Boehm, C.; Engle, A.; Neubert, A. D.; Wasvary, J. M.; Stephan, Z. F.; Steele, R. E. Synthesis and structure−activity relationships of oxamic acid and acetic acid derivatives related to L-thyronine. *J. Med. Chem.* **1995**, *38*, 695−707.
(24) Baxter, J. D.; Goede, P.; Apriletti, F. W.; West, B. L.; Feng, W.; Mellström, K.; Fletterick, R. J.; Wagner, R. L.; Kushner, P. J.; Ribeiro, R. C. J.; Webb, P.; Scanlan, T. S.; Nilsson, S. Structure-based design and synthesis of a thyroid hormone receptor (TR) antagonist. *Endocrinology* **2002**, *143*, 517−524.
(25) Evans, D. A.; Katz, J. L.; West, R. Synthesis of diaryl ethers through copper-promoted arylation of phenols with arylboronic acids. An expedient synthesis of thyroxine. *Tetrahedron Lett.* **1998**, *39*, 2937−2940.
(26) Salamonczyk, G. M.; Oza, V. B.; Sih, C. J. A concise synthesis of thyroxine (T_4) and 3,5,3′-triiodo-L-thyronine (T_3). *Tetrahedron Lett.* **1997**, *38*, 6965−6968.
(27) Entwistle, I. D.; Johnston, R. A. W.; Povall, T. J. Selective rapid transfer-hydrogenation of aromatic nitro compounds. *J. Chem. Soc., Perkin Trans. 1* **1975**, *1*, 1300−1301.
(28) Ishikawa, F.; Saegusa, J.; Inamura, K.; Sakuma, K.; Ashida, S. H. I−I. Cyclic guanidines. 17. Novel (N-substituted amino)imidazo[2,1-*b*]quinazolin-2-ones: water-soluble platelet aggregation inhibitors. *J. Med. Chem.* **1985**, *28*, 1387−1393.
(29) Anwer, M. K.; Sherman, D. B.; Roney, J. G.; Spatola, A. F. Applications of ammonium formate catalytic transfer hydrogenation. 6′ Analysis of catalyst, donor quantity, and solvent effects upon the efficacy of dechlorination. *J. Org. Chem.* **1989**, *54*, 1284−1289.
(30) Carlsson, B.; Singh, B. N.; Temciuc, M.; Nilsson, S.; Li, Y.-L.; Mellin, C.; Malm, J. Synthesis and preliminary characterization of a novel antiarrhythmic compound (KB130015) with an improved toxicity profile compared with amiodarone. *J. Med. Chem.* **2002**, *45*, 623−630.
(31) Barkhem, T.; Carlsson, B.; Simons, J.; Moeller, B.; Berkenstam, A.; Gustafsson, J. Å.; Nilsson, S. High level expression of functional full-length human thyroid hormone receptor β1 in insect cells using a recombinant baculovirus. *J. Steroid Biochem. Mol. Biol.* **1991**, *38*, 667−75.
(32) Schults, J. R.; Ruppel, P. I.; Johnson, M. A. *Biopharmaceutical statistics for drug development*; Peace, K. E., Ed.; Dekker: New York, 1988; pp 21−82.
(33) Alksnis, M.; Barkhem, T.; Stroemstedt, P. E.; Ahola, H.; Kutoh, E.; Gustafsson, J. Å.; Poellinger, L.; Nilsson, S. High level expression of functional full length and truncated glucocorticoid receptor in Chinese hamster ovary cells. Demonstration of ligand-induced down-regulation of expressed receptor mRNA and protein. *J. Biol. Chem.* **1991**, *266*, 10078−10085.
(34) Barkhem, T.; Carlsson, B.; Nilsson, Y.; Enmark, E.; Gustafsson, J.-Å.; Nilsson, S. Differential response of estrogen receptor β and estrogen receptor to partial estrogen agonists/antagonists. *Mol. Pharmacol.* **1998**, *54*, 105−112.
(35) Friedman, J. S.; Cofer, C.; Anderson, C. L.; Kushner, J. A.; Gray, P. P.; Chapman, G. E.; Lazarus, L.; Shine, J.; Kushner, P. J. High expression in mammalian cells without amplification. *Biotechnology* **1989**, *7*, 359−362.
(36) Berger, J.; Hauber, J.; Hauber, R.; Geiger, R.; Cullen, B. R. Secreted placental alkaline phosphatase: a powerful new quantitative indicator of gene expression in eukaryotic cells. *Gene* **1988**, *66*, 1−10.
(37) Southern, P. J.; Berg, P. Transformation of mammalian cells to antibiotic resistance with a bacterial gene under control of the SV40 early region promoter. *J. Mol. Appl. Genetics* **1982**, *1*, 327−341.
(38) Gritz, L.; Davies, J. Plasmid-encoded hygromycin B resistance: the sequence of hygromycin B phosphotransferase gene and its expression in *Escherichia coli* and *Saccharomyces cerevisiae*. *Gene* **1983**, *25*, 179−188.
(39) Otwinowski, Z.; Minor, W. Processing X-ray diffraction data collected in oscillation mode. In *Methods in Enzymology*; Carter, C. W., Jr., Sweets, R. M., Eds.; Academic Press: New York, 1997; vol. 276, pp 307−326.
(40) Leslie, A. G. W. Recent changes to the MOSFLM package for processing film and image plate data. CCP4 and ESF-EACMB. *Newslett. Protein Crystallogr.* **1992**, *26*.
(41) Collaborative Computational Project 4. The CCP4 suite: programs for protein crystallography. *Acta Crystallogr.* **1994**, *D50*, 760−763.
(42) Brünger, A. T.; Adams, P. D.; Clore, G. M.; DeLano, W. L.; Gros, P.; Grosse-Kunstleve, R. W.; Jiang, J. S.; Kuszewski, J.; Nilges, M.; Pannu, N. S.; Read, R. J.; Rice, L. M.; Simonson, T.; Warren, G. L. Crystallography & NMR system: A new software suite for macromolecular structure determination. *Acta Crystallogr.* **1998**, *D54*, 905−21.
(43) Jones, T. A.; Zou, J. Y.; Cowan, S. W.; Kjeldgaard, M. Improved methods for building protein models in electron density maps and the location of errors in these models. *Acta Crystallogr.* **1991**, *A47*, 110−119.
(44) Laskowski, R. A.; MacArthur, M. W.; Moss, D. S.; Thornton, J. M. PROCHECK: a program to check the stereochemical quality of protein structures. *J. Appl. Crystallogr.* **1993**, *26*, 283−291.
(45) Kraulis, P. J. Molscript: a program to produce both detailed and schematic plots of protein structures. *J. Appl. Crystallogr.* **1991**, *24*, 946−950.
(46) Merritt, E. A.; Bacon, D. J. Raster3D: photorealistic molecular graphics. *Methods Enzymol.* **1997**, *277*, 505−524.

JM021080F